Performance of Multi-hop Whisper Cognitive Radio Networks

Quanjun Chen*, Chun Tung Chou*, Salil S. Kanhere*, Wei Zhang†, Sanjay K. Jha*

*School of Computer Science and Engineering,
The University of New South Wales, Sydney, Australia,
Email: {quanc, ctchou, salilk, sanjay}@cse.unsw.edu.au

†School of Electrical Engineering and Telecommunications,
The University of New South Wales, Sydney, Australia,
Email: w.zhang@unsw.edu.au

UNSW-CSE-TR-0917

October 2009

Abstract

In 2003, Federal Communications Commission (FCC) has released a new spectrum policy called “Interference Temperature model” to improve the channel access opportunities of secondary users. Under this model, the secondary users are allowed to access the licensed spectrum simultaneously with the primary users provided that the interference at the primary receiver meets a certain threshold. We refer the Cognitive Radio Networks that employs this model as “Whisper CRNs” (since secondary users have to use smaller transmission power to satisfy the interference constraint). In this work, we systematically analyze the performance of whisper CRNs and compare it with the traditional CRNs, where the secondary users are not allowed to transmit when primary users are busy. We aim to answer the fundamental question: what is the performance trade-off by switching to whisper CRNs from traditional CRNs. Based on the performance analysis, we also propose an efficient channel assignment scheme that has a small channel switching overhead. The results show that whisper CRNs can improve the connectivity and end-to-end throughput of secondary users considerably (by more than two times in some scenarios) but at the cost of increasing end-to-end delay. We also show that the node density of secondary users has a significant impact on the performance of whisper CRNs.

I. Introduction

With the rapid growth of wireless applications, one of the main challenges that wireless communications face is the wireless spectrum scarcity. The unlicensed spectrum band, e.g., the ISM band, has become crowded with the growing popularity of WiFi and Bluetooth. On the other hand, the licensed spectrum bands have been shown to be under-utilized [1]. Cognitive radio networks (CRNs) have been proposed to solve the spectrum inefficiency problem [2].

CRNs allow secondary users to opportunistically utilize the spectrum band licensed to primary users given that the secondary users will not interfere with the primary users. In a conventional cognitive radio network, the secondary users only use the spectrum bands that are currently not occupied by the primary users in order to ensure zero interference.

However, due to the spatial reuse feature of radio signal, the licensed band can possibly be concurrently reused by the secondary users even when the primary users are busy. In fact, the Federal Communications Commission (FCC) has proposed a scheme called Interference Temperature (IT) model. In this model, the secondary users are allowed to simultaneously utilize the licensed channel with the primary users, but under the condition that the signal interference at the primary receiver is below a threshold [3]. This model clearly enhances the channel access opportunities and therefore improves the capacity of secondary users.

In interference temperature model, the secondary users must reduce their transmission power so as to meet the interference constraints at the primary users. Due to the reduced transmission power, a secondary source may not reach the destination directly (especially in a large network), which will often lead to multi-hop communications. We call such network with possibly reduced transmission power as “Whisper CRNs”. In literature, several work [4], [5], [6] have studied the performance of CRNs under interference temperature model. However, most of these work have assumed that the secondary source can communicate with the secondary destination directly even with the reduced transmission power, which can only be applied to a small size network.

In this paper, we systematically investigate the performance of whisper CRNs in a large scale ad-hoc scenario. We aim to answer the following fundamental questions: what is the performance trade-off using whisper CRNs compared to the traditional CRNs where the secondary users are not allowed to transmit when the primary users are busy?

For the multi-hop communication of secondary users, we consider a greedy geographic routing at the network layer. Greedy geographic routing is a well known localized routing scheme considered by

many routing protocols [7], [8], [9]. The underlying principle of greedy routing involves selecting the next hop from amongst a node's neighbors, which is geographically closest to the destination. Since, the forwarding decision at a node is only based on the node's local topology (i.e., location information of one-hop neighbors of this node), greedy routing is highly scalable and particularly robust to frequent changes in the network topology.

We analyze the performance of greedy geographic routing in whisper CRNs, including path availability, end-to-end throughput, and end-to-end delay. Path availability measures the probability that a source can successfully find a routing path to a destination (equivalent to connectivity).

The main contributions of this work are three-fold,

- We show that whisper CRNs can significantly improve the path availability and the end-to-end throughput of secondary users (by more than two times in some scenarios), and quantify the increase in the end-to-end delay.
- We show that the node density has a great impact on the performance of whisper CRNs. There exists a critical density range. Inside the range, we can improve the throughput significantly by deploying more secondary nodes (therefore increasing node density). However, outside the critical density range, further increase of node density will not increase the end-to-end throughput.
- Based on the analytical model, we propose an efficient channel assignment model for multiple channel CRNs, which requires the minimum channel switching overhead at secondary nodes.

The rest of paper is organized as the following. We introduce the system model in Section II. Since the hop count from a secondary source to a destination is a key element to evaluate the performance, we analyze the hop count of a secondary communication pair in Section III. We then proceed to analyze the performance of whisper CRNs in Section IV, followed by the comparison between whisper CRNs and traditional CRNs in Section V. We further propose a channel assignment scheme in Section VI. The related work is discussed in Section VII. Finally, Section VIII concludes the paper.

II. Whisper CRNs: System & physical layer models

Our CRNs consist of two types of users: primary and secondary. Primary users have the right to access its licensed spectrum while secondary users are required to ensure that the reception of primary users are not affected. In order to analytically study the performance of CRNs, we assume a 2-dimensional network. The methodology described in this paper can readily be extended to 3-dimension except that the computational requirement will be higher. Fig. 1 depicts a typical example of our CRN. We assume that the primary transmitter (node m) and primary receiver (node n) are fixed at certain locations. The

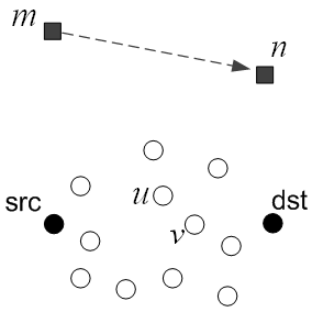

Fig. 1. Typical example of CRN considered in this paper. We use squares to represent primary users and circles to represent secondary users.

secondary nodes are assumed to be randomly distributed according to a homogenous Poisson point process with a density of ρ nodes per unit area.

At the physical layer, we assume the following radio propagation model: If the transmission power of node z is P_z, then the radio power at a distance of d from node z is given by $\frac{P_z}{d^\alpha}$ where α is the path-loss exponent; typical values of α is in the range of $[2, 6]$. Both the primary and secondary receivers will require a minimum signal-to-interference noise ratio (SINR) in order to decode the radio message. We use γ and β to denote, respectively, the minimum SINR required by the primary and secondary receivers to correctly receive the message.

There are two different modes that a CRN can operate. In the *normal* or *white space* mode, a secondary user can only access the licensed spectrum if the primary user is *idle*. However, in the *whisper* or *grey space* mode, a secondary user can access the licensed spectrum even if the primary user is *busy*, provided that, the SINR at the primary receivers remain above the decoding threshold γ. A consequence of this is that in the whisper mode, the secondary transmitter may need to reduce its transmission power in order that to guarantee that the SINR at the primary receiver is above the decoding threshold γ. Because of the reduction in transmission power in whisper mode, a secondary source may require *multi-hop* transmissions to reach its destination. This paper aims to compare the *routing* performance trade-offs of these two modes of operations. In order to realize this goal, we first analyze the region of coverage of a secondary transmitter in whisper mode. Table I contains a summary of the notation that are used in this paper.

1) Transmission coverage in whisper mode: In the absence of the primary users, a secondary transmitter will be able to reach all the nodes within its transmission range, which is a circular disk centered at the secondary transmitter. However, this situation changes when the primary user is present in a whisper

CRN, since the secondary transmitter must adjust its power to guarantee the reception of the primary receivers. This section studies the transmission coverage of secondary transmitters in whisper mode.

TABLE I

NOTATION LIST

Variables	Definition
r	Channel bandwidth (data rate)
ρ	Node density of secondary users
ε	Quantization interval
α	Path loss rate
γ, β	Minimum SINR required by the primary and secondary receivers to correctly receive the message respectively.
N_0	Noise level
m, n	Primary transmitter and primary receiver respectively
u, v or X	Secondary users
P_z	Transmission power of node z
(x_z, y_z)	(x, y)-coordinates of a point or node z
$d_{u,v}$	Euclidean distance between node u and node v
R	Radio range of the circular radio coverage of a secondary user
$P_{(x_0,y_0)->(x,y)}$	State transition probability from (x_0, y_0) to (x, y)
H (h) and $\overline{H}$	Hop count and mean hop count from a secondary source to a secondary destination respectively
$\overline{\delta}$	Average hop distance from a source to a destination
V	Path availability from a source to a destination
E	Average end-to-end throughput from a source to a destination
D	Average end-to-end delay from a source to a destination

Consider the situation depicted in Fig. 1 where nodes m and n are, respectively, the primary transmitter and receiver. We consider the communication of a pair secondary users where nodes u and v, are, respectively, the secondary transmitter and receiver. We also introduce the following notation: (1) P_z is the transmission power of node z; (2) $d_{.,.}$ will be used to denote the distance between 2 nodes, e.g. $d_{m,v}$ denotes the distance between the primary transmitter m and the secondary receiver v; (3) N_0 is the noise

power at the receivers.

The key idea of the whisper mode is that the secondary transmitter adjusts its transmission power so that both the primary and secondary pairs can communicate simultaneously. In order for this to occur, both of the following conditions must hold at the same time:

$$\frac{\frac{P_m}{d_{m,n}^{\alpha}}}{\frac{P_u}{d_{u,n}^{\alpha}} + N_0} \geq \gamma \tag{1}$$

$$\frac{\frac{P_u}{d_{u,v}^{\alpha}}}{\frac{P_m}{d_{m,v}^{\alpha}} + N_0} \geq \beta \tag{2}$$

The above two equations ensure that both the primary and secondary receivers have sufficient SINR to decode the signal. We can re-write equation (1) as

$$P_u \leq d_{u,n}^{\alpha} \left(\frac{P_m}{\gamma d_{m,n}^{\alpha}} - N_0 \right) \tag{3}$$

Assuming (i) P_m is fixed, and (ii) The locations of m, n and u, are fixed; then equation (3) imposes an upper bound on the transmission power of the secondary transmitter. Note that we can readily extend this analysis when multiple primary receivers are present. In this case, the power of the secondary transmitter will be constrained by multiple versions of Eq. (3), one for each primary receiver. In this paper, we will restrict our analysis to a single primary receiver but note that the analysis can be readily extended to the multiple primary receiver case. From this point onwards, we assume that the secondary transmitter will use the maximum allowed power, given by the right-hand-side of Eq. (3), to reach its receiver.

Consider Eq. (2) and note that the only quantity that we can vary in the equation is the location of the secondary receiver v, we can therefore use this equation to determine the region $\mathcal{C}$ in which a secondary receiver v should lie in order for it to be able to decode the signal from the secondary transmitter u. In other words, the region $\mathcal{C}$ is the *transmission coverage* of the secondary transmitter in whisper mode. We will abuse the notation and use v to denote the location of the node v too. We can define the region $\mathcal{C}$ as:

$$\mathcal{C} = \{v : \frac{\frac{P_u}{\beta}}{d_{u,v}^{\alpha}} - \frac{P_m}{d_{m,v}^{\alpha}} \geq N_0\} \tag{4}$$

Note that the set membership definition in (4) is obtained from rearranging Eq. (2). Note that the exact shape of the coverage region $\mathcal{C}$ is unknown except when $N_0 = 0$, $\mathcal{C}$ is an Apollonius Circle [10] with foci at nodes m and u. We will show that $\mathcal{C}$ can be well approximated by a circle centred at the point C with radius R, whose expressions will be given in a moment. Note that (x_u, y_u) will be used to denote the (x, y)-coordinates of a point or node u.

The center C of the circle, which we will use to approximate $\mathcal{C}$, is at (x_c, y_c), where

$$\begin{aligned} x_c &= x_u + \frac{(x_u - x_m)(d_2 - d_1)}{2\sqrt{(x_u - x_m)^2 + (y_u - y_m)^2}} \\ y_c &= y_u + \frac{(y_u - y_m)(d_2 - d_1)}{2\sqrt{(x_u - x_m)^2 + (y_u - y_m)^2}}, \end{aligned} \tag{5}$$

and the radius of the circle is

$$R = \frac{d_1 + d_2}{2} \tag{6}$$

where d_1 and d_2 are the solutions of the following two equations:

$$\frac{\frac{P_u}{\beta}}{d_1^\alpha} - \frac{P_m}{(d_{m,u} - d_1)^\alpha} - N_0 = 0 \tag{7}$$

$$\frac{\frac{P_u}{\beta}}{d_2^\alpha} - \frac{P_m}{(d_{m,u} + d_2)^\alpha} - N_0 = 0 \tag{8}$$

Fig. 2 compares the actual shape of area $\mathcal{C}$ with the approximation of the circle defined in Eq. (5) and (6). We assume that node u and m are located at $(0, 0)$ and $(0, 500)$ respectively, and $\frac{P_u}{\beta} = 0.05W$, $P_m = 0.5W$, $\alpha = 3$. Since the difference between the approximation and the actual region is mainly determined by the noise power N_0, we vary N_0 from 1.0e-12W (low noise level) to 1.0e-07W (high noise level). Fig. 2(a) and 2(d) illustrate that the approximated circle is identical to the actual region when the noise power is either very low (e.g. N_0 =1.0e-12W) or very high (e.g. N_0 =1.0e-07W). For the medium level of noise power, there is a only slight difference between the approximation and the true region, as shown in Fig. 2(b) and 2(c). We have tested different network parameters and similar patterns are observed as Fig. 2. Overall, our extensive numerical results show that our approximations are very close to the actual regions of $\mathcal{C}$.

Fig. 3 depicts the meaning of d_1 and d_2 in this approximation. The distances d_1 and d_2 are the distances from the secondary transmitter u to the two ends of the diameter of the circle that lies on the line connecting m and u. It is interesting to point out that the center of the coverage region of a secondary transmitter is no longer at the transmitter itself. The center is displaced in the direction from the primary transmitter m to secondary transmitter u. The cause of this can be explained as follows: Since a secondary receiver requires a minimum SINR to decode the signal, the receivers that are closer to the primary transmitter will experience a higher interference and may not be able to decode the signal. Therefore, the coverage is displaced in the direction away from the primary user.

The above discussion shows that the radio coverage of a secondary user depends on the locations of the secondary user, primary transmitter and primary receiver. Now we illustrate the radio coverage of a secondary user using numerical results calculated by Eq. (6) We assume $P_m = 27dBm$, $N_0 = -90dBm$,

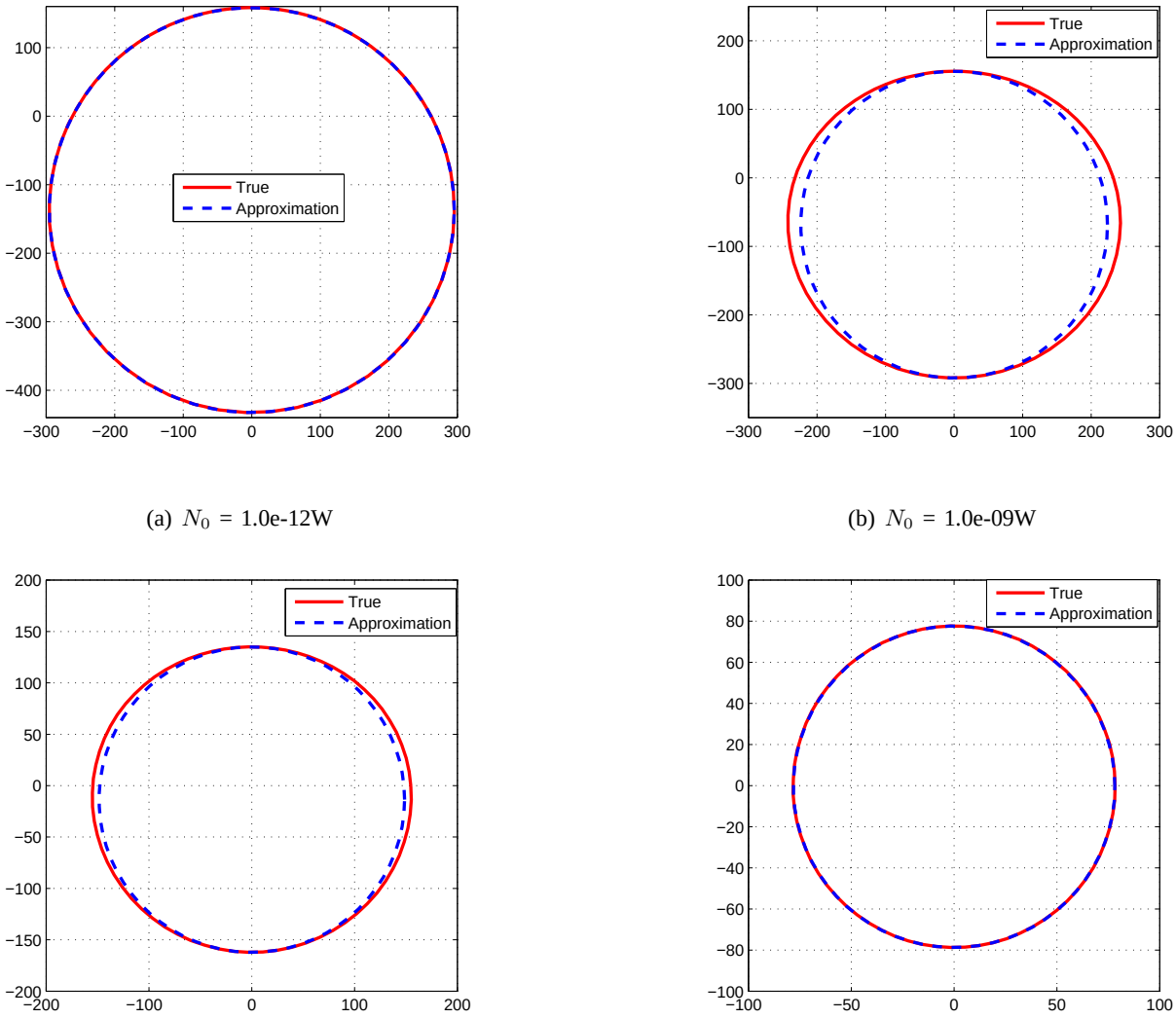

(a) N_0 = 1.0e-12W

(b) N_0 = 1.0e-09W

(c) N_0 = 1.0e-08W

(d) N_0 = 1.0e-07W

Fig. 2. Approximation of the radio coverage of the secondary user

$\alpha = 3$, $\gamma = \beta = 11.76dB$, and the primary transmitter and receiver are located at (0,500) and (500,500) respectively. Fig. 4 shows the radio range R of a secondary user whose location varies along the line connecting (0,0) to (500,0). The figure shows that the radio range decreases first but after a certain point the radio range goes up. This is caused by the two conflicting factors. On one hand, when the secondary user is closer to the primary receiver (and therefore further away from the primary transmitter), it should use a smaller transmission power due to the interference constraint at primary receiver, which results in a smaller radio range. On the other hand, when the secondary user is further away from the primary

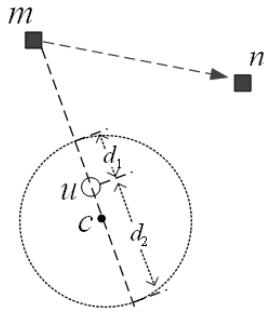

Fig. 3. Illustration of radio coverage of a secondary node.

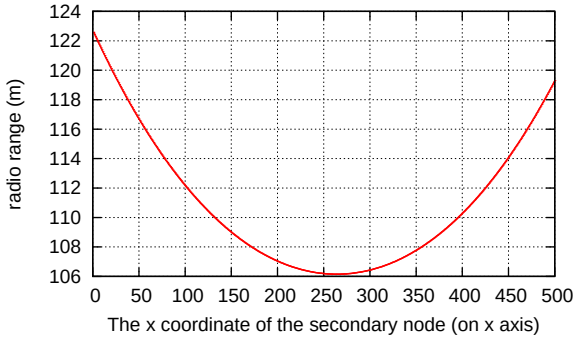

Fig. 4. Radio range as a function of the location of the secondary node.

transmitter, it experiences less interference from the primary transmitter, which may lead to larger radio range. Therefore, the decrease in Fig. 4 is due to the dominant effect of the first factor but increase is due to the presence of the second factor.

Given this transmission coverage analysis of the secondary user, we are now ready to use it as a basis to analyse the multi-hop routing performance in a whisper CRN.

III. Analysis of Hop Count

Recall that, in whisper CRNs, the secondary users have to reduce their transmission powers to protect the transmission of primary users, which can lead to multi-hop communications. This section seeks to develop a model for analyzing the hop count from the secondary source to the secondary destination in a whisper CRN when the primary users are busy. We use a discrete Markov chain to model the hop-by-hop progress of a packet from the source to the destination. The state of the Markov chain is defined as the location of the current forwarding node that holds the packet. Consider the network in Figure 5 where the node X located at (x_0, y_0) is currently holding the packet. Let us assume that node X chooses

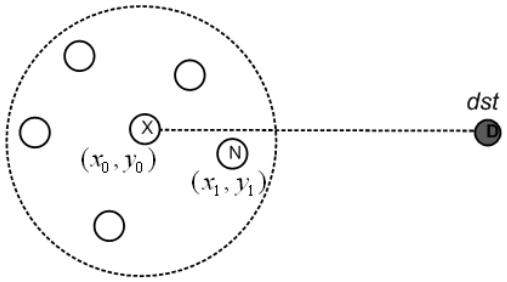

Fig. 5. Network to illustrate state transition.

node N located at (x_1, y_1) as the next hop. We model this packet movement from nodes X to N as a state transition from (x_0, y_0) to (x_1, y_1). In general, the hop-by-hop progress, that is made by a packet towards the destination, can be represented by a series of state transitions that eventually culminates in state (x_d, y_d), which are the coordinates of the destination D.

Note that ideally the states in this Markov chain should be modeled as a continuous random variable. However, to simplify our model, we use a discrete state space to approximately represent the continuous values. We divide the two-dimensional network area into a grid, each cell of which has a length of ε and a width of ε, where the parameter ε is the interval of the state space (i.e. the quantization coefficient). When the interval ε is small enough, the discrete state space approximates the original continuous space.

Our analysis is composed of the following steps. The first step involves determining the state transition probabilities for the Markov chain (section III-A) using geometric calculation. Based on the transition probabilities, we recursively compute the hop count distribution and the mean value given a communication pair (Section III-B). Finally, we propose an approximation to simplify the analysis and reduce the computational complexity (Section III-C).

A. State Transition Probability

The aim of this section is to derive an expression for the state transition probability, which will be used in the next section to derive a probability density function of the hop count for greedy geographic routing in whisper CRN. In greedy routing, a forwarding node selects the next hop from amongst its neighbors (i.e. the set of nodes within its coverage) that is geographically closest to the destination. If multiple neighbors have the same closest distance to the destination, the forwarding node randomly selects one as the next hop.

We will illustrate this by considering the situation depicted in Fig. 6. Node X is the secondary

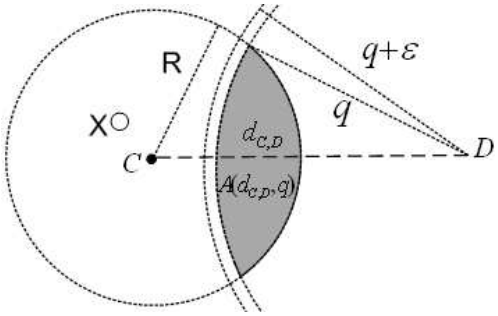

Fig. 6. Illustration to prove state transition probability.

transmitter that currently holds the packet. The circle is the coverage region of node X when the primary transmitter is busy. Note that the location of the centre C and the radius R of the coverage region are functions of the location of X as well as those of the primary users, and for brevity, we will not make this dependence explicit. We assume that the next state is at a location that is distance q away from the destination D. Since we assume a discrete state space with ε as the quantization interval, we can approximate all the locations that are at distance q from the destination as a thin trip with the thickness of ε, as illustrated in Fig. 6. The shaded area in Fig. 6 contains all the points that are in the transmission coverage of X and are at distance of no more than q from the destination D. Following the rule of selecting the next hop in geographic routing, the node X will select a node in the thin strip (which is a distance of $[q, q+\varepsilon]$ from the destination D and is within the coverage of node X) in Fig. 6 as the next hop if there is no secondary node in the shaded region. Since, if there exists a secondary node in the shaded region, then this node will be closer to the destination than any node in the thin strip, so any node in the thin strip will not be chosen. Therefore, the probability that current node X will send the packet to a node within the thin strip is the same as the probability of the joint event that there are no secondary nodes in the shaded region and there is at least a node in the thin strip. We have the following theorem.

Theorem 1: We assume that the current state of the packet be (x_0, y_0), which corresponds to a secondary transmitter X situated at this location. Let C and R be, respectively, the location of the centre and the radius of the coverage region of node X. Let $d_{X,D}$ and $d_{C,D}$ denote the distance from, respectively, X and C, to the destination D. In whisper mode, the transition probability of a packet from

current state (x_0, y_0) to (x, y) (which is at a distance q from the destination D) is:

$$P_{(x_0,y_0)->(x,y)} = \begin{cases} 1 & \text{if } d_{C,D} \leq R \text{ and } q = 0, \\ \eta(d_{C,D}, q) & \text{if } d_{C,D} > R \text{ and} \\ & d_{C,D} - R \leq q < d_{X,D}, \\ 0 & \text{otherwise} \end{cases} \tag{9}$$

where

$$\begin{aligned} \eta(d_{C,D}, q) &= \frac{\exp(-\rho A(d_{C,D}, q)) - \exp(-\rho A(d_{C,D}, q+\varepsilon))}{A(d_{C,D}, q+\varepsilon) - A(d_{C,D}, q)} \\ A(d_{C,D}, q) &= R^2 \arccos \frac{{d_{C,D}}^2 + R^2 - q^2}{2 d_{C,D} R} \\ &\quad + q^2 \arccos \frac{{d_{C,D}}^2 + q^2 - R^2}{2 d_{C,D} q} \\ &\quad - \frac{\sqrt{((R + d_{C,D})^2 - q^2)(q^2 - (R - d_{C,D})^2)}}{2} \end{aligned} \tag{10}$$

△△△

Proof: Note that the physical meaning of the term $A(d_{C,D}, q)$ is the area of the shaded region in Fig. 6, which is the intersection of the coverage region of node X and a circle of radius q centered at the destination D.

In general, the transition probability from X (located at (x_0, y_0)) to any location that is at distance q from the destination, denoted as $P_{(x_0,y_0)->q}$, is the probability that at least one node lies inside region $A(d_{C,D}, q+\varepsilon) - A(d_{C,D}, q)$ (which is the thin strip mentioned in the paragraph before the theorem) and there are no nodes within $A(d_{C,D}, q)$. Since the secondary nodes are Poisson distributed with density ρ, this probability is given by $\exp(-\rho A(d_{C,D}, q)) - \exp(-\rho A(d_{C,D}, q+\varepsilon))$. The transition probability to a particular location (x, y) within this thin ring is $P_{(x_0,y_0)->q}$ divided by the area of the thin strip. This explanation covers the second case of Eq. (9), where the next state is within the radio coverage of node X and is closer to the destination D than node X.

For the first case in Eq. (9), where $d_{C,D} \leq R$, the destination node is within the radio coverage of the current node X. Hence, if the next state under consideration is at the destination (i.e. $q = 0$), node X will forward its packets to the destination directly with probability of 1. For all other cases, e.g. the next hop (x, y) is outside the radio coverage of node X, the transition probability is zero. △△△

B. Hop Count Distribution and Mean Value

Based on the transition probability computed earlier and using recursive computation, we have the following results on the probability density function of the hop counts.

Theorem 2: Given a secondary source node S (located at (x_s, y_s)) and a destination D (at (x_d, y_d)), let C and R denote respectively the centre and radius of the coverage region of the source S. Furthermore, let $d_{C,D}$ denotes the distance between C and D. The probability distribution of hop count H (a discrete random variable) in greedy routing for whisper CRNs is given by:

$$P(H = h|(x_s, y_s), (x_d, y_d)) = \begin{cases} 1 & \text{if } h = 1 \text{ and } d_{C,D} \leq R, \\ 0 & \text{if } h = 1 \text{ and } d_{C,D} > R, \\ \xi & \text{if } h > 1 \end{cases} \tag{11}$$

where

$$\xi = \sum_{(x,y)} P_{(x_s,y_s)->(x,y)} P(H = h - 1|(x, y), (x_d, y_d)) \tag{12}$$

and $P_{(x_s,y_s)->(x,y)}$ is the state transition probability given in Theorem 1. △ △△

Proof: Note that if the hop count from the current state (x_s, y_s) to the destination is h, then hop count from the next state (x, y) to the destination must be $h - 1$. By applying the law of total probability, we have the recursive Eq. (12). For probability of $h = 1$ (i.e. one hop), the probability is 1 if the destination node is within the coverage of the source node S (which occurs if $d_{C,D}$ is less than R), otherwise the probability is zero. △ △△

The result of Theorem 2 shows that we can use recursive computation to obtain the probability density function of the hop-count for a given secondary source-destination pair. We can use the hop count density function to derive *path availability* and *mean hop count.*

1) Path availability: Note that, there is a certain chance that an intermediate forwarding node may not be able to find the next hop (i.e. no neighbor is closer to the destination than the forwarding node itself), the greedy routing fails in such case as it cannot find a routing path [1]. In fact, for a given pair of source and destination, if we sum the hop count probabilities over all hop count values, the result is the probability that the source can successfully find a routing path to the destination. We denote the summation as V, and refer it as the *path availability* from the source S to the destination D. We have,

$$V = \sum_{h=1}^{\infty} P(H = h|(x_0, y_0), (x_d, y_d)) \tag{13}$$

[1]In a conventional geographic routing protocol, other forwarding schemes, e.g. face routing [7], are used when the greedy routing fails. We do not consider these recovery schemes for simplicity.

2) Mean hop count: Now we proceed to compute the mean hop count for a given communicating pair. Note that, the hop count is only meaningful when there is a routing path from the source to the destination. Therefore, when we calculate the mean hop count, we only consider the case that the source can successfully find a routing path to the destination.

Based on Theorem 2, the probability that the hop count is h is $P(H = h|(x_0, y_0), (x_d, y_d))$. Consequently, the probability that the hop count is h on the condition that there is a routing path, is $P(H = h|(x_0, y_0), (x_d, y_d))/V$. Finally, the mean hop count $\overline{H}$ on the condition that there is a routing path is:

$$\overline{H} = \frac{\sum_{h=1}^{\infty} h \cdot P(H = h|(x_0, y_0), (x_d, y_d))}{V} \tag{14}$$

3) Example: We illustrate the mean hop count given by Eq. (14) using a numerical example. We assume that the secondary destination is located at (500, 0). The primary transmitter and receiver are located at (0,500) and (500,500) respectively. The unit of the $x - y$ coordinates is meter. Node density is $\rho = 0.0002$ per square meters. The quantization interval is $\varepsilon = 1m$. Fig. 7 shows the mean hop count from the different source locations to the destination. The level of grey at a location indicates the mean hop count from this location to the destination. This figure clearly shows the impact of primary pair on the hop count. Note that, in a traditional wireless ad hoc network (no primary users), when the source is further away from the destination, it generally takes longer hops to reach to the destination [11]. However, Fig. 7 shows that this rule does not hold when there exists power constraints and interference due to primary users. For example, although location A in the figure (364m from the destination) is closer to the destination than the location B (412m from the destination), a node at location A takes more hops (5.8 hops) to reach the destination than the source at location B (4.3 hops). This is due to the non-uniform transmission power of the secondary users. In this example, location A is closer to the primary receiver, it is forced to use a smaller transmission power in order to satisfy the interference constants at the primary receiver. A smaller transmission power leads to a smaller radio coverage and therefore more hops to reach the destination.

Note that, the above computation of the mean hop count requires us to recursively compute the hop count distribution at each location in the entire 2-dimensional space. This computation has a time complexity of $O(d^3)$, where d is the distance between the source and destination. It is evident that evaluating the mean hop count for a sizable network can be a considerably computationally intensive task. Hence, in the next section, we derive a simplified technique to estimate the mean hop count.

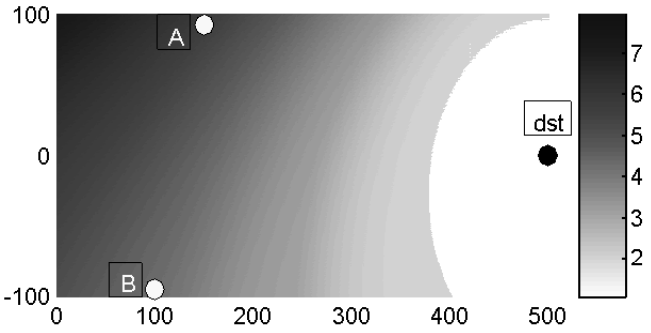

Fig. 7. Mean hop count as a function of source location. The destination is located at (500,0). Primary transmitter and primary receiver are located at (0,500) and (500,500) respectively.

C. Approximation of Mean Hop Count

In order to compute the mean hop count approximately, we introduce the concept of *hop distance*, which measures how far the packet can progress towards the destination in one hop. If we can estimate the average hop distance along the routing path, denoted as $\overline{\delta}$, we can approximate the mean hop count as the ratio of the source-to-destination distance to the average hop distance.

$$\overline{H} = \frac{d_{(x_s,y_s),(x_d,y_d)}}{\overline{\delta}} \tag{15}$$

In order to calculate the average hop distance along the routing path, we need to know the hop distance when the packet is at any intermediate location (x, y). This can be derived from the state transition probability presented in Theorem 1. Let $d_{0,D}$ be the distance from the current location (x_0, y_0) to the destination, and $d_{n,D}$ be the distance from the next state (x, y) to the destination. The hop distance can be calculated by:

$$\delta(x_0, y_0) = \sum_{(x,y)} (d_{0,D} - d_{n,D}) P_{(x_0,y_0)->(x,y)} \tag{16}$$

It is noteworthy that the mean hop count is the average hop count on the condition that there is a routing path from the source to the destination. Similarly, when we calculate hop distance, we should also consider the condition that each intermediate forwarding node can successfully find a next hop. Let $W(x_0, y_0)$ be the probability that a node at location (x_0, y_0) can successfully find the next hop, referred as *link success probability*. According to greedy routing, $W(x_0, y_0)$ is the probability that at least one neighbor of the node is closer to the destination than the node itself. Based on the geometric calculation, we have

$$W(x_0, y_0) = 1 - \exp(-\rho A(d_{C,D}, d_{C,D})) \tag{17}$$

where $d_{C,D}$ is the distance from the center of transmission coverage of the node located at (x_0, y_0) to the destination, and the expression for the function $A(\cdot,\cdot)$ is given in Theorem 1.

Therefore, the hop distance at (x_0, y_0) given that next hop exists is:

$$\delta(x_0, y_0) = \frac{\sum_{(x,y)}(d_{0,D} - d_{n,D})P_{(x_0,y_0)->(x,y)}}{W(x_0, y_0)} \tag{18}$$

However, due to the non-uniform radio coverage of secondary users, the hop distance at each intermediate node is different. In other words, when a packet makes its way to the destination, the hop distance it experiences at each hop varies. Under this observation, we further assume that all the intermediate forwarding nodes are located along the straight line connecting the source and destination [2]. Therefore, the average hop distance is the average value of hop distance over all the locations along the routing path. Let Ω be the set of locations that lies on the straight line connecting the source and destination. We have,

$$\overline{\delta} = \frac{\sum_{(x,y)\in\Omega} \delta(x, y)}{\sum_{(x,y)\in\Omega} 1} \tag{19}$$

As an illustration, we compare the approximation of mean hop count with the exact calculation via Eq. (14). We assume the same network parameters as used in Fig. 7. Fig. 8 shows the mean hop count when the source varies from location (0,0) to (0,500) (along the x axis). Note that the destination is fixed at (0,500) in this example. The figure shows that the simplified calculation can approximate the mean hop count with an error of less than 17%. However, the computation complexity is reduced significantly from $O(d^3)$ to $O(d)$ since the recursive computation is now carried out along a line, rather than on a plane.

IV. Performance Analysis When Primary Users Are Busy

In this section, we analyze the end-to-end performance of a secondary communication pair in whisper mode, i.e. when the primary users are busy. We first define the performance metrics, including path availability, end-to-end delay and end-to-end throughput. We then investigate impact of network parameters on the performance of secondary network, including the parameters of secondary source-to-destination distance, the distance from secondary pair to primary pair and the nodes density.

[2]The actual forwarding nodes in greedy routing are around the straight line connecting the source and the destination.

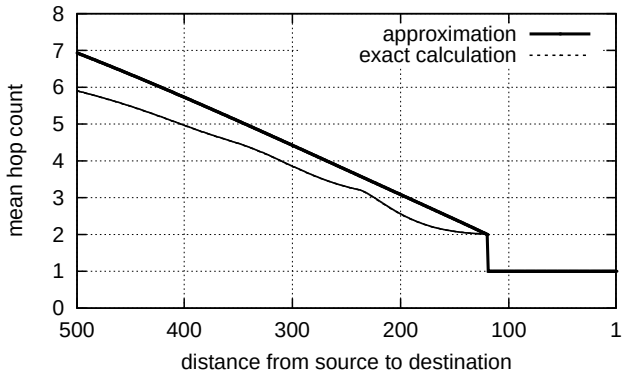

Fig. 8. Approximation of mean hop count as a function of source-to-destination distance

A. Path Availability

Path availability measures the probability that a source can successfully find a routing path to a destination. As discussed in Section III-B, path availability can be calculated by the hop count distribution according to Eq. ((13)). However, this approach requires a high computation complexity due to the requirement of hop count distribution information. Here, we also propose a simplified approach to estimate the path availability. Recall that, when a packet is making its way to the destination, each intermediate node may fail to find the next hop. Path availability is the joint probability that all the forwarding nodes (including the source) can successfully find a next hop. We use $W(x, y)$ to denote the probability that an intermediate node at location (x, y) can successfully find the next hop. If we know the average value of W over all intermediate nodes, and the mean hop count $\overline{H}$, we can estimate the path availability for the whisper mode by

$$V_{whisper} = \overline{W}^{(\overline{H}-1)} \tag{20}$$

In above equation, we only consider $\overline{H} - 1$ hops because that the forwarding node at the last hop always has a direct connection to the destination. therefore, the link successful probability at last hop is always 1.

Similar to the approximation of mean hop count, we assume that all the intermediate forwarding nodes lie in the straight line connecting the source and destination. Therefore, an approximation for the mean per-hop availability is

$$\overline{W} = \frac{\sum_{(x,y)\in\Omega} W(x, y)}{\sum_{(x,y)\in\Omega} 1} \tag{21}$$

where Ω has the same meaning as that in Section III-C.

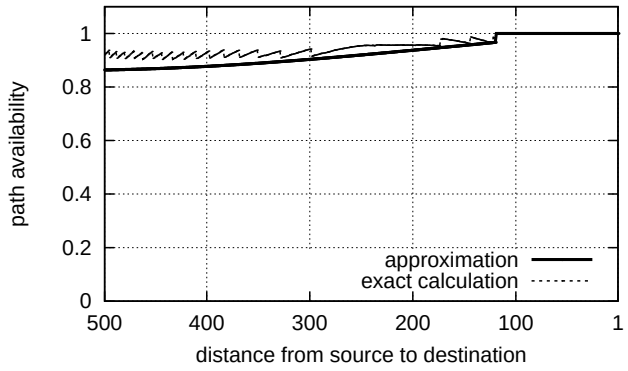

Fig. 9. Approximation of path availability as a function of source-to-destination distance

Fig. 9 illustrates the comparison between the exact calculation of path availability with the approximation. We assume the same network parameters as those for Fig. 7. Fig. 9 shows the path availability when the source varies from location (0,0) to (0,500) (along the x axis). Note that, the destination is fixed at (0,500) and therefore the distance from the source to the destination varies from 500 to 0. Fig. 9 shows that the approximation is close to the actual mean hop count. Similar to the the approximation of mean hop count, the computation complexity is reduced significantly from $O(d^3)$ to $O(d)$.

B. End-to-End Delay

The wireless transmission at each hop introduces some delay, including packet processing delay, propagation delay, queuing delay. The end-to-end delay generally is proportional to the hop count from the source to the destination. Assume that the average delay at each hop is t_d. The average end-to-end delay of a communication pair when there is a routing path, is

$$D_{whisper} = \overline{H} \cdot t_d \tag{22}$$

C. End-to-End Throughput

We assume that, when a secondary user transmits a packet, all the other secondary nodes keep silent (i.e. no spatial reuse is applied among secondary users)[3]. We further assume that there is only one

[3]Note that, if we consider the channel reuse, multiple secondary users can utilize the channel at the same time. Therefore, we need a power allocation algorithm to assign power for each of the multiple transmitters so that their collective interference at the primary receive is below the required constraint. We also need a multi-access protocol for collision avoidance between 1-2 hop neighbours. We plan to address this issue in our future work.

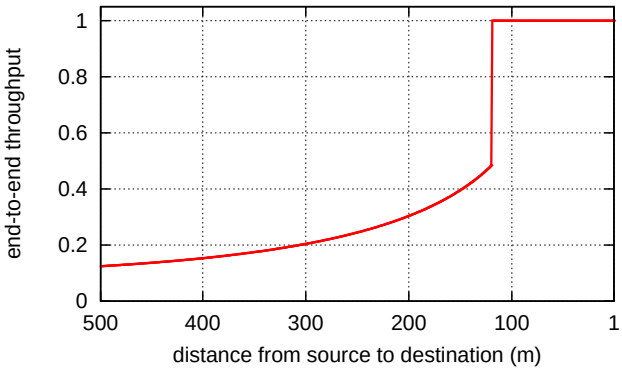

Fig. 10. Impact of secondary source-to-destination distance on the end-to-end throughput

communicating pair in the network. Under these simplified assumption, the throughput of the pair is the data rate at link layer r divided by the hop count from the source to the destination, i.e. $\frac{r}{H}$. (Note that, we assume that the secondary nodes use a constant transmission rate r at the link layer. One can think of this as the transmission rate that can be supported by SINR threshold β of the secondary users.) Note that, when the source cannot find a routing path to the destination, the throughput is zero. Therefore, the average end-to-end throughput, E, is

$$E_{whisper} = \frac{r}{H} \cdot V \tag{23}$$

where V is the path availability probability.

Now we study the impact of network parameters on the end-to-end throughput of secondary pair using numerical results from Eq. (23). We vary the parameters, including the distance from secondary source to secondary destination, the distance from the primary pair to secondary pair and finally the node density. The primary transmitter and the primary receiver are fixed at (0,500) and (500,500) respectively.

We first vary the distance between the secondary source and the secondary destination. We fix the destination at location (500,0) and vary the source from (0,0) to (500,0). Other parameters are the same as those in preparing Fig. 7. We normalize the end-to-end throughput using the link data rate r. Fig. 10 shows the numerical results of the normalized end-to-end throughput as the function of source-to-destination distance. It illustrates that, when the primary user is busy, the secondary throughput is quite low for a larger source-to-destination distance. It then increases slowly with the distance, until the two nodes are so close that the source can directly communicate with the destination even with the reduced transmission power. Generally, secondary pair can gain great benefit from the whisper mode when the secondary source is close to the destination.

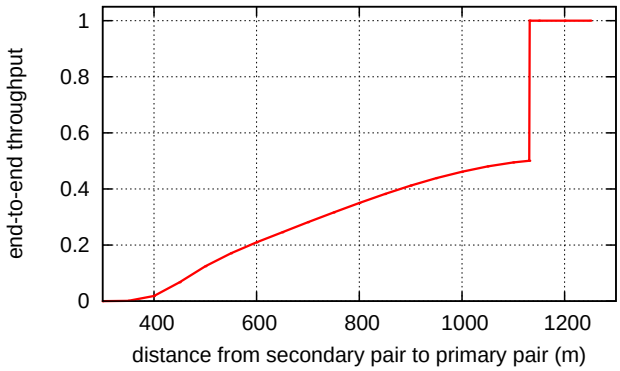

Fig. 11. Impact of distance from the primary pair to the secondary pair on the end-to-end throughput

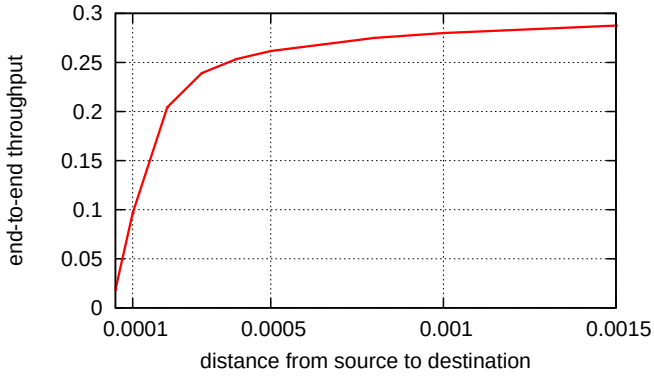

Fig. 12. Impact of node density on the end-to-end throughput

In the second study, we vary the distance between the primary and secondary pairs. The primary transmitter and receiver are still fixed at (0,500) and (500,500) respectively (the primary pair is parallel to the x-axis). The secondary source and destination are also 500m apart, and are placed in a line parallel to x axis but we vary the y-coordinate of the secondary pair from 200 to -800. Equivalently, the distance from the primary pair to the secondary pair varies from 300m to 1300m. Fig. 11 depicts that throughput increases linearly with the distance initially. After a certain point (distance of 1150m), the secondary pair is so far away from the primary pair that the transmitting power limitation due to the interference constraint disappears. As a result, the secondary source can use the maximum allowed transmission power and communicate with the secondary destination directly. Therefore, secondary pair can achieve a better performance when secondary pair is located far away from the primary pair.

Recall that, node density has a great impact on the path availability and therefore end-to-end throughput

(according to Eq. (23)). Next, we study the actual impact of nodes density on the throughput. We vary the node density ρ from 0.0001 to 0.0015. The source and the destination is located at $(200, 0)$ and $(500, 0)$ respectively. Fig. 12 shows the end-to-end throughput as a function of node density. It shows that the throughput increases rapidly with an increase in the node density, but the rate of increase slows down considerably before it converges to a maximum value. In other words, there exists a critical density range. Inside the range, we can improve the throughput dramatically by deploying more secondary nodes (therefore increasing node density). However, outside the critical density range, further increase of node density will not benefit the end-to-end throughput.

V. Traditional CRNs versus whisper CRNs

In this section, we compare the performance of traditional CRNs with whisper CRNs. In a traditional CRN, a secondary user is only allowed to transmit when the primary user is idle. A whisper CRN operates in two modes. When the primary user is present, the secondary users operate in the whisper mode and reduce their transmission power to ensure that the primary receivers are not affected. When the primary user is idle, the secondary users operate in a normal mode, which is identical to the traditional CRN. Without loss of generality, our analysis considers the case that a secondary source-destination pair can communicate in one hop when the primary user is idle.

When analysing the performance of whisper CRNs, we need to take into account its two modes of operation. We have analysed the performance, in terms of path availability, throughput and delay, of the whisper mode in Section IV. In normal mode, where the primary user is idle, the secondary source can reach the destination in one hop. Therefore, the path availability is 1, the throughput is the link rate r and the delay is t_d. By combining these results, we have:

Proposition 1: Let τ be the fraction of time that primary user is busy. For whisper CRNs, the path availability is:

$$V = (1 - \tau) + \tau V_{whisper} \tag{24}$$

the average end-to-end throughput is,

$$E = (1 - \tau) \cdot r + \tau E_{whisper} \tag{25}$$

and the average end-to-end delay is

$$D = (1 - \tau) \cdot t_d + \tau D_{whisper} \tag{26}$$

For traditional CRNs, the path availability is $V = (1 - \tau)$, the average end-to-end throughput is $E = (1 - \tau) \cdot r$ and the average end-to-end delay is $D = t_d$. $\triangle\ \triangle\triangle$

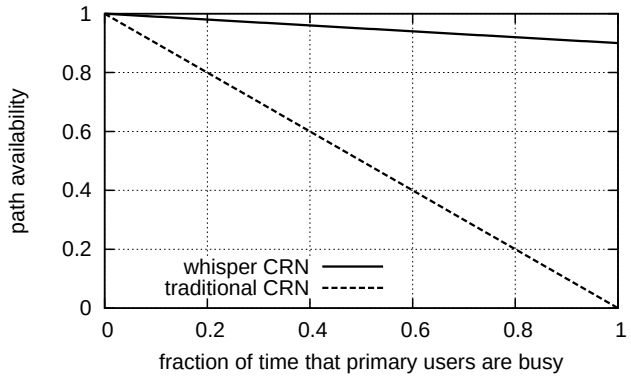

Fig. 13. Comparison of path availability between whisper CRN and white CRN.

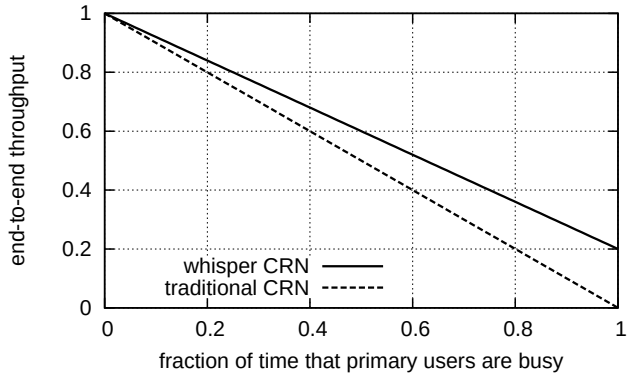

Fig. 14. Comparison of throughput between whisper CRN and white CRN.

We use a numerical example to compare the performance of whisper and traditional CRNs based on above proposition. The network parameters are the same as those used in Fig. 7. The secondary source and the destination are located, respectively, at $(200, 0)$ and $(500, 0)$. Fig. 13 compares the path availability of whisper and traditional CRNs. The figure shows that whisper CRN can improve the path availability significantly especially if the primary user has a high probability of being busy.

Fig. 14 compares the end-to-end throughput of the whisper CRNs and the traditional CRNs. We normalize the throughput by the link data rate r. It shows that the improvement in throughput increases with the fraction of time that primary users are busy. For example, if the primary users are busy 80% of time, then the throughput of the whisper CRNs is almost twice that of the traditional CRNs. Note that if the primary user is always busy, the throughput of traditional CRNs is zero but a whisper CRN can maintain a throughput equal to about 20% of link rate.

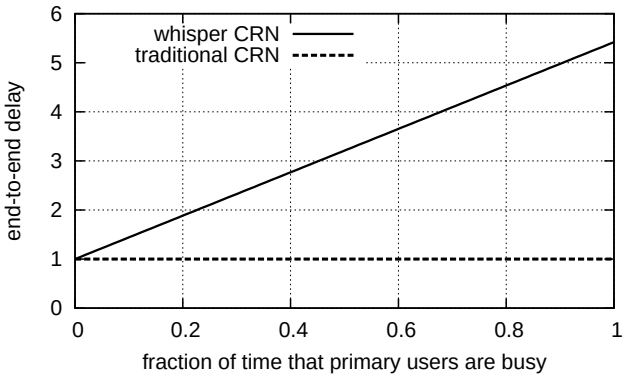

Fig. 15. Comparison of delay between whisper CRN and white CRN.

Fig. 15 compares the end-to-end delay between the whisper CRN and traditional CRN. We normalize the end-to-end delay to the one hop delay t_d. Fig. 14 shows that whisper CRN actually introduces significant delay compared to the traditional CRN, due to the multi-hop communications. However, note that, for traditional CRNs, we have not included the time that, if a packet arrives while the primary user is busy, the time it takes for the primary user to become idle. This ”residual waiting” time can only be computed if we make additional assumptions on packet arrival patterns and primary user usage patterns. We note that this can be large if the primary user is busy for a large proportion of the time.

Figures 13, 14 and 15 show that whisper CRN can improve the path availability and throughput compared with traditional CRNs. The price that one has to pay for using whisper CRN is a possibly long delay due to multi-hopping. However, this delay can be reduced if a packet can utilise different channels on its way from the secondary source to destination.

VI. Multi-channel whisper CRNs

Our analysis on the performance of whisper CRNs has assumed only one channel. The analysis in the last Section shows that a whisper CRN can improve both path availability and throughput. However, the delay in a whisper CRN can be long because of multi-hopping since the secondary nodes must reduce their transmission power when the primary user is busy. Note that in our earlier analysis also shows that the number of hops is also a function of hop distance, which is in turn a function of the locations of the primary users and secondary users. Therefore, if multiple orthogonal channels are available and if the primary users operating in these channels are situated at different locations, a secondary user can choose a channel to maximise the end-to-end performance. In this section, we propose and analyse a channel assignment strategy, which works in conjunction with greedy geographic routing.

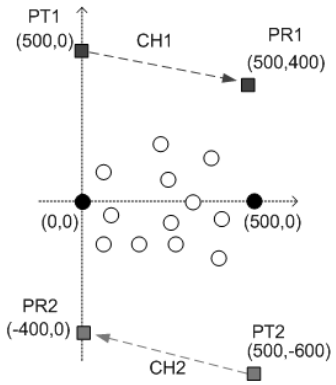

Fig. 16. Example for two primary pairs.

In order to simplify the description, we consider the case with 2 channels. The proposed scheme can be extended to more than two channels. We also assume that both channels have the same link layer data rate. Consider the situation depicted in Fig. 16 where two primary user pairs operate in two channels: channels 1 and 2. Note that, in Fig. 16, the primary receiver of channel 1 is closer to the secondary destination than it is to the secondary source. If a packet is routed to the destination from the source using channel 1 only, as the packet gets closer to the primary receiver, the nodes holding the packets are forced to use a smaller transmission range because they must reduce their transmission power in order not to affect the primary receiver. In order words, the hop distance in channel 1 becomes smaller as it gets closer to the destination. On the other hand, the primary receiver of channel two is closer to the secondary source than it is to the secondary destination. Therefore, if the packet is routed using channel 2 when it is near the destination, then the nodes holding the packet can use a larger transmission range, or longer hop distance. This can improve the end-to-end performance.

We confirm the intuitive argument in the last paragraph by plotting the hop distances of intermediate nodes when using different channels in Fig. 17. The hop distance is calculated by Eq. (16). Similar to the approximate procedure to compute the mean hop count, we assume that the intermediate nodes are located along the straight line from the source to the destination. Fig. 17 shows that there exists a cut off point. To the left side of this point, using channel 1 will give a large hop distance but to the right side of this point, using channel 2 instead will give a larger hop distance.

This motivates us to propose a channel assignment strategy which can readily work with greedy geographic routing. The channel assignment strategy determines a cut-off point between the source and the destination, where the nodes on the two sides of the point (also referred as left segment and right

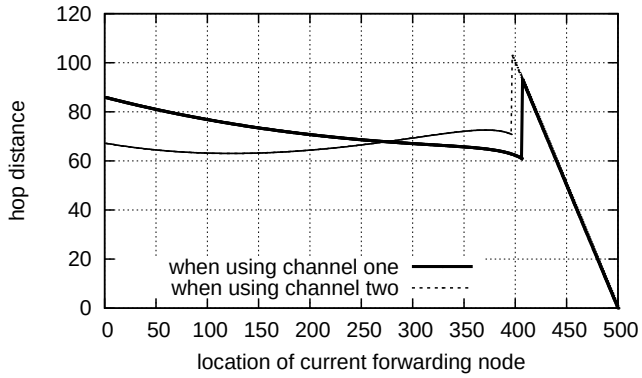

Fig. 17. Hop distance as a function of nodes' location.

segment) use different channels simultaneously. Note that we continue to assume that only one secondary communication can take place in one channel. However, the two different channels are assumed to be orthogonal, the communications on these two channels can occur at the same time. The outline of the channel assignment strategy is proposed below:

1) The source calculates the optimal cut-off point and the channel assignment for both sides of the cut-off point, based on the network parameters and the location of destination.
2) When the source formats the packet, it puts the location of the cut-off point, as well as the channel assignments on both sides of the cut-off point, in the packet header.
3) Upon receiving a packet, the intermediate node compares its location to the cut-off point. If it is on the left side of the cut-off point, it uses the channel assigned for the left segment, and vice versa.

We now discuss how the source can find the optimal cut-off point for a given communicating pair. Since we can use the two channels simultaneously, the segment that has larger hop count becomes the performance bottleneck. As a result, the end-to-end throughput is determined by the segment that has larger hop count. Let h^l and h^r be, respectively, the average hop count of the left and right segments. The end-to-end throughput is $r/\max\{h^l, h^r\}$ [4]. If we want to maximize the end-to-end throughput, we need to choose the channel combination that minimizes the the larger hop count of two segments, i.e. $\min(\max\{h^l, h^r\})$.

We use w to denote the location of the cut-off point, i.e. the cut-off point is at a distance of w from the secondary source. Let $h_1^l(w)$, $h_2^l(w)$ be the average hop count of left segment when using channel

[4]Here we assume that node density is high enough so that the path availability is 1. Therefore, the end-to-end throughput is only a function of hop count.

one and channel two respectively. Similar, let $h_1^r(w)$, $h_2^r(w)$ be the average hop count of right segment when using channel one and channel two respectively.

The value of $h_1^l(w)$ can be estimated by the mean hop count approximation procedure discussed in Section. III-C. Note that the use of the approximation procedure reduces the computation burden at the source. We have,

$$h_1^l(w) = \frac{w}{\frac{\sum_{(x,y)\in\Omega^l} Q_1(x,y)}{\sum_{(x,y)\in\Omega^l} 1}} \tag{27}$$

where $Q_1(x,y)$ is the hop distance of a node at location (x,y) when using channel one, and Ω^l is the set of discrete location points between the source and the cut-off point.

Similar for $h_2^r(w)$, we have

$$h_2^r(w) = \frac{D-w}{\frac{\sum_{(x,y)\in\Omega^r} Q_2(x,y)}{\sum_{(x,y)\in\Omega^r} 1}} \tag{28}$$

Let $T(w,1)$ be the end-to-end throughput of secondary pair if we split the routing path at w with the left segment uses channel 1 and the right segment uses channel 2. We have,

$$T(w,1) = \frac{r}{\max\{h_1^l(w), h_2^r(w)\}} \tag{29}$$

The optimal end-to-end throughput is

$$T(1) = \max_w T(w,1) \tag{30}$$

and the optimal cut-off point for this channel assignment is:

$$w_1 = \arg\max_w T(w,1) \tag{31}$$

Similarly, let $T(w,2)$ be the end-to-end throughput of secondary pair if we split the routing path at w with the left segment uses channel 2 and the right segment uses channel 1.

The optimal end-to-end throughput for this particular channel assignment is:

$$T(2) = \max_w T(w,2) \tag{32}$$

and the optimal cut-off point is

$$w_2 = \arg\max_w T(w,2) \tag{33}$$

Therefore, if $T(1) \geq T(2)$, we should assign channel 1 to the left segment and channel 2 to the right segment, and use w_1 as the cut-off point. Otherwise, we assign channel 2 to the left segment and channel 1 to the right segment, and use w_2 as the cut-off point.

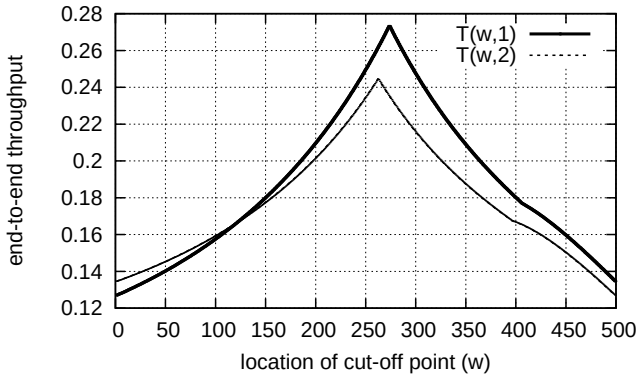

Fig. 18. End-to-end throughput as a function of cut-off point.

For an illustration, Fig. 18 shows the numerical results of the normalised throughput $T(w,1)$ and $T(w,2)$ as a function of w. The normalisation is done with the link data rate r. The network parameters are the same as those used in preparing Fig. 17. Fig. 18 shows that, when using the channel 1 in the left segment, we can achieve the maximum throughput $T(1) = 0.27r$ if the cut-off point is at 273. On the other hand, if we use the channel 2 in the left segment, we can achieve the maximum throughput $T(2) = 0.24r$ when the cut-off point is at 262. Since $T(1)$ is larger than $T(2)$, we should assign channel 1 to the left segment and use 273 as the optimal cut-off point. In this example, if we only use one channel for all intermediate nodes from the source to the destination, the best throughput that we can only achieve is $0.12r$. Therefore, by using this channel assignment, we can actually double the end-to-end throughput.

Note that, in this assignment, all intermediate nodes at the left side of cut-off point use the same channel, and the same for the right side segment. Consequently, only the secondary link that crosses over the cut-off point needs to perform channel switching operation (assume one radio interface is equipped at each secondary user). Therefore, our channel assignment can actually achieve the minimum channel switch overhead.

VII. Related Work

In this section, we provide an overview of related work on the interference temperature model in CRN. In [12], the authors present a primer on the IT model, its advantages and research challenges. In [5], the author analyzes the capacity achieved by the secondary network assuming that secondary transmitters communicate with a common base station. The same author in [6] also proposes a Media Access Control (MAC) protocol to utilize interference temperature model. Zhang in [4] studies the achievable capacity

assuming fading channels. The author considers two cases of interference constraints. One is that the average interference of secondary transmitter over all the fading states at the primary receiver should be below the threshold. The second constraint assumes that the peak interference at each fading state is below the threshold.

In whisper CRNs, multiple secondary users may utilize the channel at the same time. Therefore, we need a power allocation algorithm to assign power for each of the multiple transmitters so that their interference sum at the primary receive is below the required constraint. The work in [13], [14] investigates optimal power control strategies for secondary users with the goal of maximising their capacity (throughput). In [15], [16], [17], [18], [19], several resource allocation schemes are presented that can satisfy the requirements of both interference constraints for primary users and the QoS constraints for secondary users.

However, all above work assume that, in a secondary pair, the secondary source can communicate with the secondary destination directly. Recall that in the IT model, the secondary users have to reduce their transmission power when the primary users are busy. This smaller transmission power may mean additional relay nodes are needed to forward packets from the source to the destination, especially in a large scale secondary network. In this study, we consider a general ad-hoc CRN where the source communicates with destination via a multi-hop communication. To the best of knowledge, this is the first work to systematically study the performance of multi-hop CRN under interference temperature model.

VIII. Conclusion

Interference temperature (IT) model allows the secondary users to simultaneously utilize the channel with the primary users, which improves the channel access opportunities of cognitive radio networks. Since the secondary users in IT model use a reduced transmission power, a secondary source may need a multi-hop communication with the destination, especially in a large scale ad-hoc CRN. In this paper, we have provided a first step to study the performance of such network. We show that the secondary users can gain benefit from IT model in several scenarios, e.g. when the secondary pairs are located far from the primary pairs. We also illustrate that node density has a great impact on the performance of secondary users. Our comparison results of whisper CRNs with traditional CRNs show that, generally, IT model can improve the connectivity and the throughput of secondary users considerably but also increase the end-to-end delay while achieving this. In this work, we have considered a localized routing protocol and proposed an efficient localized channel assignment. In the future, we are going to investigate other advanced routing, MAC protocols or channel assignment schemes, and use the the performance results

presented in this work as a comparison baseline for future work.

REFERENCES

[1] FCC. Spectrum policy task force report. ET Docket No. 02-135, November 2002.

[2] I. F. Akyildiz, W.-Y. Lee, and K. R. Chowdhury. Crahns: Cognitive radio ad hoc networks. *Ad Hoc Netw.*, 7(5):810–836, 2009.

[3] FCC. Notice of inquiry and notice of proposed rulemaking. ET Docket No. 03-237, November 2003.

[4] R. Zhang. On peak versus average interference power constraints for spectrum sharing in cognitive radio networks. In *The 3rd IEEE Symposium on New Frontiers in Dynamic Spectrum Access Networks DySPAN.*, pages 1–5, October 2008.

[5] T. C. Clancy. Achievable capacity under the interference temperature model. In *INFOCOM 2007: Proceedings of the 26th Annual IEEE Conference on Computer Communications*, pages 794–802, May 2007.

[6] T. Charles Clancy. Dynamic spectrum access using the interference temperature model. *Annals of Telecommunications*, 64(7-8):573–592, August 2009.

[7] B. Karp and H. T. Kung. GPSR: Greedy perimeter stateless routing forwireless networks. In *Proceedings of the 6th Annual International Conference on Mobile Computing and Networking*, pages 243–254, Boston, MA, USA, August 2000.

[8] H. Luo, F. Ye, J. Cheng, S. Lu, and L. Zhang. TTDD: Two-tier data dissemination in large-scale wireless sensor networks. *Wireless Networks*, 11:161–175, March 2005.

[9] S. Ratnasamy, B. Karp, L. Yin, F. Yu, D. Estrin, R. Govindan, and S. Shenker. GHT: a geographic hash table for data-centric storage. In *WSNA 2002: Proceedings of the 1st ACM International Workshop on Wireless Sensor Networks and Applications*, pages 78–87, Atlanta, GA, USA, September 2002.

[10] C. S Ogilvy. *Excursions in Geometry*. Dover, 1990.

[11] Q. Chen, S. S. Kanhere, and M. Hassan. Hop count analysis for greedy geographic routing. UNSW-CSE-TR-0824, ftp://ftp.cse.unsw.edu.au/pub/doc/papers/UNSW/0824.pdf, 2008.

[12] P. J. Kolodzy. Interference temperature: a metric for dynamic spectrum utilization. *International Journal of Network Management*, 16(2):103–113, 2006.

[13] W. Wang, T. Peng, and W. Wang. Optimal power control under interference temperature constraints in cognitive radio network. In *Wireless Communications and Networking Conference, 2007.WCNC 2007. IEEE*, pages 116–120, March 2007.

[14] H. Li, Y. Gai, Z. He, K. Niu, and W. Wu. Optimal power control game algorithm for cognitive radio networks with multiple interference temperature limits. In *Vehicular Technology Conference, 2008. VTC Spring 2008. IEEE*, pages 1554–1558, May 2008.

[15] L. Le and E. Hossain. Resource allocation for spectrum underlay in cognitive radio networks. *IEEE Transactions on Wireless Communications*, 7:5306–5315, December 2008.

[16] D. I. Kim, L. Le, and E. Hossain. Joint rate and power allocation for cognitive radios in dynamic spectrum access environment. *IEEE Transactions on Wireless Communications*, 7:5517–5527, 2008.

[17] D. I. Kim W. J. Shin, K. Y. Park and J. W. Kwon. Large-scale joint rate and power allocation algorithm combined with admission control in cognitive radio networks. *Journal of Communications and Networks*, 11(2):157–165, April 2009.

[18] Y. Xing, C. N. Mathur, M. A. Haleem, R. Chandramouli, and K. P. Subbalakshmi. Dynamic spectrum access with qos and interference temperature constraints. *IEEE Transactions on Mobile Computing*, 6(4):423–433, April 2007.

[19] B. Yang, Y. Shen, G. Feng, C. Long, Z.-P. Jiang, and X. Guan. Distributed power control and random access for spectrum sharing with qos constraint. *Computer Communication*, 31(17):4089–4097, 2008.